

Polaronic nature of a muonium-related paramagnetic center in SrTiO₃

T. U. Ito,^{1, a)} W. Higemoto,^{1, 2} A. Koda,³ and K. Shimomura³

¹⁾Advanced Science Research Center, Japan Atomic Energy Agency, Tokai, Ibaraki 319-1195, Japan

²⁾Department of Physics, Tokyo Institute of Technology, Meguro, Tokyo 152-8551, Japan

³⁾Institute of Materials Structure Science, High Energy Accelerator Research Organization (KEK), Tsukuba, Ibaraki 305-0801, Japan

(Dated: 24 October 2019)

The hyperfine features and thermal stability of a muonium (Mu)-related paramagnetic center were investigated in the SrTiO₃ perovskite titanate via muon spin rotation spectroscopy. The hyperfine coupling tensor of the paramagnetic center was found to have prominent dipolar characteristics, indicating that the electron spin density is dominantly distributed on a Ti site to form a small polaron near an ionized Mu⁺ donor. Based on a hydrogen-Mu analogy, interstitial hydrogen is also expected to form such a polaronic center in the dilute doping limit. The small activation energy of 30(3) meV found for the thermal dissociation of the Mu⁺-polaron complex suggests that the strain energy required to distort the lattice is comparable to the electronic energy gained by localizing the electron.

Electron doping into an archetypal perovskite titanate, SrTiO₃, results in intriguing physical properties such as superconductivity¹ and ferromagnetism,² and can help form a two-dimensional (2D) electron gas system at the LaAlO₃/SrTiO₃ heterointerface.^{3,4} This makes electron-doped SrTiO₃ a promising material for emerging oxide electronics. For many of its applications, it is crucial to determine whether excess electrons form either free or trapped carriers. However, experimental studies on (La, Nb)-doped or oxygen-deficient SrTiO₃ seem contradictory on this point. Optical conductivity and dc transport measurements showed that excess electrons behave as free carriers or large polarons having band-like characteristics.^{5,6} On the other hand, photoemission spectroscopy (PES) studies revealed an incoherent in-gap state, which can be associated with small polarons, and its coexistence with a coherent delocalized state.⁷ The Kondo effect observed in an electric field-effect-induced 2D electron system in SrTiO₃ also suggests the coexistence of free and trapped carriers.⁸ Although many theoretical studies have been conducted to understand such puzzling phenomena,^{9–11} the origin of the dual electron behavior in *n*-type SrTiO₃ remains unclear.

Interstitial hydrogen (H_i) also serves as a shallow donor in SrTiO₃.¹² PES measurements on a SrTiO₃ (001) *surface* exposed to hot atomic hydrogen showed both in-gap and delocalized states.¹³ This implies that small polarons can also exist in H_i-doped SrTiO₃. However, little is known about the microscopic nature of hydrogen dopants and doped electrons in *bulk* SrTiO₃ except for some insight provided by infrared (IR) and polarized Raman scattering spectroscopies^{14–16} and positive muon spin rotation (μ⁺SR) spectroscopy.^{17,18} Further experimental investigations are required to fully elucidate the role of H_i in *bulk* SrTiO₃ and better understand the behavior of excess electrons in *n*-type SrTiO₃.

Since hydrogen and muonium (Mu: a μ⁺-e⁻ bound state) have almost the same reduced mass, the μ⁺SR technique has been extensively used for the study of hydrogen-related defects in condensed matter.^{17–23} In this letter, we report a detailed μ⁺SR study in bulk SrTiO₃, focusing on the electronic structure of a Mu-related paramagnetic defect that results from muon implantation. Only two μ⁺SR studies on SrTiO₃ have been published to date.^{17,18} These reported shallow Mu⁰-like features with ionization energies of several tens of meV and hyperfine coupling parameters in the MHz range. Salman *et al.* performed measurements at 25 K in a zero applied field (ZF) and transverse fields (TFs) below 12 mT and obtained a fully anisotropic hyperfine coupling tensor for the Mu⁰-like center.¹⁸ However, the physical identity of the paramagnetic center is far from being fully elucidated. In this study, we carefully evaluated the hyperfine coupling tensor at 1.7 K under TFs above 0.1 T. This tensor showed prominent dipolar characteristics, suggesting that the electron spin density is dominantly distributed on a Ti site adjacent to an interstitial muon (Mu_i⁺) bound to an O²⁻ ion. Such a feature indicates that the small polaron can also form in “Mu-doped” bulk SrTiO₃ near an ionized Mu_i⁺ donor. Our temperature variation study revealed that the Mu_i⁺-polaron complex easily dissociates at moderate temperatures with an activation energy of 30(3) meV. Similar small polarons bound to positively charged impurities may explain the dual behavior of excess electrons observed in other electron-doped SrTiO₃ systems.^{7,8}

A nominally undoped SrTiO₃ single crystal of 10×10×0.5 mm³ was obtained from Furuuchi Chemical Co., Japan. The single crystal was grown by the Verneuil method and cut along the cubic (001) plane. It is worth mentioning that we did not actively control the domain distribution in an antiferro-distortive (AFD) phase below 105 K. Hence, we use cubic notation to specify crystallographic directions for both cubic and pseudocubic-AFD phases. μ⁺SR experiments were

^{a)}ito.takashi15@jaea.go.jp

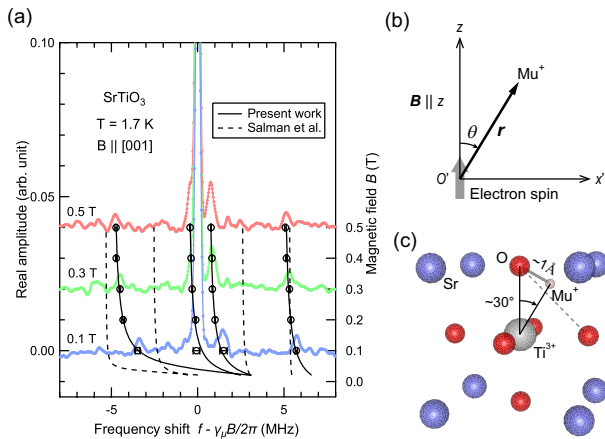


FIG. 1. (a) FT- μ^+ SR spectra at 1.7 K in TFs of 0.1, 0.3, and 0.5 T applied along the [001] direction (small solid circles with lines). The left vertical axis and the horizontal axis correspond to the real Fourier amplitude and the frequency shift $f - \gamma_\mu B/2\pi$, respectively. The B dependences of paramagnetic frequency shifts are also shown with large open circles. The right vertical axis represents B . The solid curves are the best fits to $f(B; \theta, A_{iso}, A_{dip})$ calculated from eqs. (1) and (2). The dashed curves are the high-field extension of paramagnetic frequency shifts calculated with hyperfine parameters in Ref. [18]. (b) Coordinate system (x', y', z) for the point-dipole model. (c) Schematic illustration of the Mu_i^+ -bound small polaron in SrTiO_3 .

performed at Paul Scherrer Institut (PSI), Switzerland, using the GPS instrument²⁴ and a spin-polarized surface muon beam in the TF configuration. The SrTiO_3 single crystal was mounted on a low-background sample holder with the (001) plane perpendicular to the muon incident direction. TFs up to 0.5 T were applied along the [001] direction. The asymmetry of the muon beta decay was monitored by the “Up” and “Down” positron counters and recorded in the temperature range 1.7-300 K.

Figure 1(a) shows the TF- μ^+ SR spectra in the frequency domain (Fourier transform (FT) spectra) at 1.7 K for several TFs. The horizontal axis corresponds to the frequency shift which is defined as $f - \gamma_\mu B/2\pi$, where f is the muon spin precession frequency, $\gamma_\mu (=2\pi \times 135.53 \text{ MHz})$ is the muon gyromagnetic ratio, and B is the magnetic field. Two pairs of satellite lines were clearly identified, indicating that a paramagnetic electron is localized near the muon and the hyperfine coupling between these particles is strongly anisotropic. The central frequencies of the four paramagnetic lines, superimposed in Fig. 1(a) as functions of B , were obtained from time domain fits to an oscillatory function composed of five exponentially-damped cosines (one for a diamagnetic line at $f = \gamma_\mu B/2\pi$). The largest principal value of the hyperfine coupling tensor was roughly estimated to be in the order of 10^1 MHz from the splitting of the outer pair. This is much smaller than the electron Zeeman frequency above 0.1 T ($>2.8 \text{ GHz}$). Hence, the z component of the electron spin operator \mathbf{s} becomes

a good quantum number. Under such conditions, two lines in each pair simply correspond to $s_z = \pm \frac{1}{2}$ states. If the hyperfine coupling is isotropic, as in the case of atomic Mu^0 , the electron spin creates a collinear hyperfine field at the muon position and the splitting should be symmetric in terms of the diamagnetic muon frequency $\gamma_\mu B/2\pi$. This is clearly not the case in SrTiO_3 , for which asymmetric shifts were observed in both satellite pairs (Fig. 1(a)). In addition, the asymmetry is more remarkable at lower B values. This strongly suggests that the hyperfine fields corresponding to the four paramagnetic lines are noncollinear to \mathbf{B} and therefore a dipolar contribution is dominant in the hyperfine coupling.²² Such a situation is expected to occur when an electron is localized primarily at a single cation in close proximity to a Mu_i^+ donor to form a polaronic center.¹⁹

To verify this hypothesis quantitatively, we analyzed the field dependences of the paramagnetic shifts using the following spin Hamiltonian \mathcal{H} ,

$$\mathcal{H}/h = \boldsymbol{\nu}_e \cdot \mathbf{s} - \boldsymbol{\nu}_\mu \cdot \mathbf{I} + (A_{iso} + \mathbf{A}_{dip})\mathbf{s} \cdot \mathbf{I}, \quad (1)$$

where $\boldsymbol{\nu}_e = |g|\mu_B \mathbf{B}/h$ is the electron Zeeman frequency, $g(\sim 2)$ is the electron g -factor; $\boldsymbol{\nu}_\mu = \gamma_\mu \mathbf{B}/2\pi$ is the muon Zeeman frequency, \mathbf{I} is the muon spin operator, A_{iso} is the isotropic hyperfine coupling constant due to the Fermi contact interaction, and \mathbf{A}_{dip} is the dipolar hyperfine coupling tensor. Here we adopt a point-dipole model to describe \mathbf{A}_{dip} in detail, where the electron spin is localized at the origin, as depicted in Fig. 1(b), and creates a dipolar field at the muon location \mathbf{r} . In the TF configuration, μ^+ SR is insensitive to the crystal rotation around the field axis along the z direction in the laboratory frame (x, y, z). To simplify the expression for \mathbf{A}_{dip} , another coordinate system (x', y', z) for the point-dipole model was selected so that the x' - z plane contains \mathbf{r} . In this frame, \mathbf{A}_{dip} is expressed as follows,

$$\mathbf{A}_{dip} = \frac{A_{dip}}{2} \begin{pmatrix} 3 \sin^2 \theta - 1 & 0 & 3 \sin \theta \cos \theta \\ 0 & -1 & 0 \\ 3 \sin \theta \cos \theta & 0 & 3 \cos^2 \theta - 1 \end{pmatrix}, \quad (2)$$

$$A_{dip} = \frac{\mu_0 \gamma_\mu |g| \mu_{eff}}{4\pi^2 r^3}, \quad (3)$$

where θ is the angle between \mathbf{B} and \mathbf{r} , μ_{eff} is the effective magnetic moment for the localized electron, and $r(=|\mathbf{r}|)$ is the electron-muon distance. With this expression a pair of paramagnetic frequencies can be calculated for each θ . A global fit to the calculated $f(B; \theta, A_{iso}, A_{dip})$ was performed for the inner and outer frequency pairs with shared A_{iso} and A_{dip} . Solid curves in Fig. 1(a) represent the best fit with $A_{iso} = 1.4(3) \text{ MHz}$, $A_{dip} = 15.5(2) \text{ MHz}$, $\theta = 33(1)^\circ$ or $180^\circ - 33(1)^\circ$ for the outer pair, and $\theta = 62(1)^\circ$ or $180^\circ - 62(1)^\circ$ for the inner pair. This point-dipole model reproduced the field-dependent asymmetric feature of the paramagnetic lines in $\mathbf{B} \parallel [001]$ well.

The hyperfine parameters ($A_{dip} \gg A_{iso}$) suggest that the spin density distribution is considerably compact and

the center of gravity of the distribution is displaced from the muon position by an atomic-scale length. This is similar to the case wherein a small polaron is trapped near an ionized donor. In titanates, the small polaron is often found in the form of a nominally Ti^{3+} (d^1) ion accompanied by a significant lattice distortion.^{7,25} Thus, we assume that an electron spin and a Mu^+ donor are respectively located on a Ti site and an interstitial site near an oxygen ion to form an OMu^- group in the same unit cell. Based on the atomic configuration around H_i^+ reported from first-principles calculations,¹¹ Mu_i^+ is expected to locate at $\theta = 29^\circ$ on a TiO_2 plane near an O-O edge of an oxygen octahedron (Fig. 1(c)). This agrees with θ for the outer paramagnetic pair and also with θ for the inner pair after a 90° -rotation of the system in the TiO_2 plane. Therefore, the two sets of satellite pairs can be assigned to the identical paramagnetic centers in different AFD domains. The Mu_i^+ site shown in Fig. 1(c) is also consistent with the H_i^+ site determined from IR and polarized Raman scattering measurements in the cubic and pseudocubic-AFD phases.¹⁴⁻¹⁶ When the Ti-H distance is considered as $r = 2.2\text{\AA}$ in eq. (3) based on a theoretical structure,¹¹ μ_{eff}/μ_B becomes $0.33(1)$, which is of order unity and therefore consistent with the characteristics of the nominally- Ti^{3+} small polaron. Thus, we conclude that the identity of the Mu^0 -like paramagnetic center is a Mu_i^+ -bound small polaron. From the Mu-H analogy, H_i in SrTiO_3 is also expected to act as an auto-ionized shallow donor that can trap one excess electron in the form of the nominally- Ti^{3+} small polaron, at least in the dilute doping limit. It is worth mentioning that a similar Mu_i^+ -polaron complex was reportedly found in rutile TiO_2 .^{22,23} However, there seems to be ambiguity as to the degree of electron localization since the hyperfine parameters for this state (~ 1 MHz) are too small to ascribe to a Ti^{3+} ion in close proximity to Mu_i^+ .

We then analyzed the thermal properties of the Mu_i^+ -bound small polaron by examining the temperature dependence of μ^+ SR spectra. Figure 2(a) shows the temperature evolution of FT- μ^+ SR spectra in a TF of 0.5 T applied along the [001] direction. As temperature increased, a decrease in the paramagnetic fraction and an increase in the diamagnetic one were observed, suggesting that thermal dissociation of the Mu_i^+ -bound small polaron occurred. To obtain a more detailed analysis of the dissociation process, we performed fits in the time domain to an exponentially-damped cosine function using data points after $3\ \mu\text{s}$, where the paramagnetic signals were mostly damped. Figure 2(b) displays the temperature dependence of the diamagnetic fraction obtained by the fits, which is qualitatively consistent with that reported in Ref. [18] under a low TF of 10 mT. We used the ionization model from Ref. [18] to fit our data and obtained a characteristic energy E_a of $30(3)$ meV. The E_a in the ionization model usually represents the depth of a shallow Mu^0 donor level measured from the conduction band minimum; however, in this case, it should be interpreted as the activation energy for the Mu_i^+ -polaron

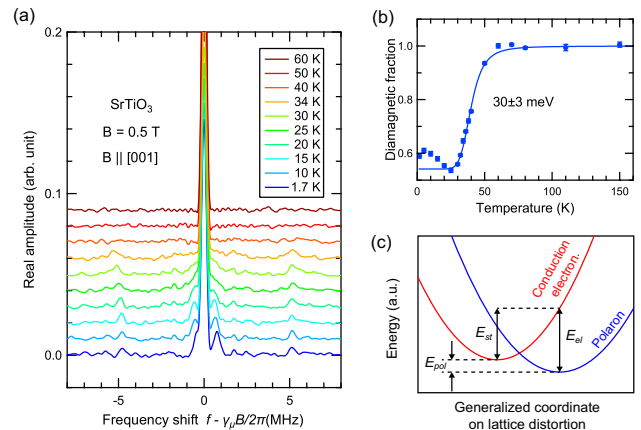


FIG. 2. (a) Temperature evolution of FT- μ^+ SR spectra in a TF of 0.5 T applied along the [001] direction. (b) Temperature dependence of the diamagnetic fraction. The solid curve represents the best fit to the ionization model for data points above 25 K. (c) Schematic illustration of the energy balance for polaron formation in the presence of lattice distortions.

dissociation. The electron separated from the Mu_i^+ donor is expected to serve as a charge carrier in the form of either a delocalized conduction-band electron or a hopping small polaron. The small E_a , comparable in magnitude with the characteristic thermal energy at room temperature, indicates that the interstitial doping of Mu (or H) into SrTiO_3 leads to n -type conductivity, which is consistent with hydrogen doping studies.¹²

The fate of the electron released from the Mu_i^+ -polaron complex depends on the nature of excess electrons in the perfect SrTiO_3 lattice. Some computational studies suggest that excess electrons in SrTiO_3 tend to delocalize rather than create self-trapped small polarons unless Coulomb and strain fields due to ionized dopants are present.^{9,10} This is in sharp contrast to the situation in rutile TiO_2 , where the stability of self-trapped small polarons has been established from both theoretical and experimental viewpoints.²⁵⁻²⁷ Thus, we assume that the electron released from the Mu_i^+ -polaron complex is immediately transferred to the conduction band in SrTiO_3 . This assumption is also consistent with the coherent delocalized state detected by PES in n -type SrTiO_3 .^{7,13} There may seem to be a disagreement between the small E_a and the highly localized nature of the small polaron, which usually forms a deep in-gap state.^{9,10,25} This could be explained by considering the energy balance for polaron formation in the presence of a lattice distortion due to the localized electron and ionized dopant,^{10,25,26} as illustrated in Fig. 2(c). The electronic energy E_{el} , associated with the deep single-particle state at ~ 1 eV below the conduction band minimum, is the quantity measured by PES or scanning tunneling spectroscopy within the time scale where lattice atoms are considered to be frozen (vertical excitation). In addition, the polaron formation energy E_{pol} is defined as the total energy difference between the polaronic and delocalized states in fully relaxed

lattices. These energies are connected through the relation $E_{pol} = E_{el} - E_{st}$ with the strain energy E_{st} required to distort the lattice. In the thermal dissociation process associated with the E_a obtained from μ^+ SR, the polaronic electron may be transferred to the conduction band via a minimum energy path in Fig. 2(c) with an energy barrier comparable to E_{pol} . The value for E_{pol} was estimated for Nb-doped SrTiO₃ to be in the range of several tens of meV by first-principles calculations.¹⁰ This is comparable in magnitude with our estimation for Mu(H)-doped SrTiO₃ in the dilute doping limit. When $E_{pol} \ll E_{el} \sim E_{st}$, strain and Coulomb fields induced by ionized dopants must play a crucial role in stabilizing the small polaron ground state.

There are some important discrepancies between this μ^+ SR study and the preceding work by Salman *et al.*¹⁸ They determined the principal values of the hyperfine coupling tensor \mathbf{A}' as 1.4(1), 6.7(1), and 11.5(1) MHz from μ^+ SR frequencies observed at 25 K in ZF. Because the dipolar part in \mathbf{A}' should be traceless, the coefficient of the isotropic part is estimated as $\text{Tr}[\mathbf{A}']/3 = 6.5(1)$ MHz, which is comparable in magnitude with the largest principal value. This implies that the muon is located in an extended electron cloud as in the case of a hydrogenic shallow donor. Contrastingly, we concluded from the $A_{dip} \gg A_{iso}$ relation at 1.7 K that the electron spin density is dominantly distributed on a Ti site adjacent to an ionized Mu_i^+ . This discrepancy may be partly due to the fact that the hyperfine parameters were investigated at different temperatures. The splitting of the paramagnetic lines seems mostly symmetric at 25 K, while it is undoubtedly asymmetric at 1.7 K (Fig. 2(a)). This change is probably attributed to the activation of *local* Mu^+ motion among four quasi-equivalent sites around the nearest $\text{Ti}^{3+}\text{-O}^{2-}$ bond in our model. In this situation, the component of the hyperfine field perpendicular to \mathbf{B} is averaged to zero and the remaining parallel component causes the symmetric splitting. In Ref. [18], TF dependences of paramagnetic frequencies at 25 K below 12 mT were analyzed with \mathbf{A}' expressed in the laboratory frame using two sets of Euler angles. The high-field extension of paramagnetic frequency shifts calculated with these parameters is shown in Fig. 1(a) (dashed lines). These parameters obviously fail to explain our experimental results at 1.7 K. Another difference is the interpretation of the small E_a . It was previously interpreted as an ionization energy of a shallow hydrogen-like Mu^0 ,¹⁸ while we assigned it to the effective binding energy of a polaronic electron stabilized near Mu_i^+ . In our model, a single-particle level associated with the well-localized electron is expected to lie deep in the band gap as observed in other electron-doped SrTiO₃ systems.^{7,13}

In conclusion, we observed a spectroscopic signature of a Mu_i^+ -bound small polaron in bulk SrTiO₃, which easily dissociates at moderate temperatures ($E_a = 30(3)$ meV). In the dilute doping limit, H_i is also expected to form such a polaronic center according to the hydrogen-Mu analogy. The direct observation of a deep in-gap state

by PES in the bulk crystal of H_i -doped SrTiO₃ would be crucial to identify the H_i^+ -bound small polaron state corresponding to the muonic one.

ACKNOWLEDGMENTS

We thank the staff of the PSI muon facility for technical assistance and K. Nishiyama and K. Fukutani for helpful discussions. This work was partially supported by Grant-in-Aid for Young Scientists (No.16K17544) from Japan Society for the Promotion of Science.

- ¹J. F. Schooley, W. R. Hosler, and M. L. Cohen, Phys. Rev. Lett. **12**, 474 (1964).
- ²W. D. Rice, P. Ambwani, M. Bombeck, J. D. Thompson, G. Haugstad, C. Leighton, and S. A. Crooker, Nat. Mater. **13**, 481 (2014).
- ³A. Ohtomo and H. Y. Hwang, Nature **427**, 423 (2004).
- ⁴K. Yoshimatsu, R. Yasuhara, H. Kumigashira, and M. Oshima, Phys. Rev. Lett. **101**, 026802 (2008).
- ⁵J. L. M. van Mechelen, D. van der Marel, C. Grimaldi, A. B. Kuzmenko, N. P. Armitage, N. Reyren, H. Hagemann, and I. I. Mazin, Phys. Rev. Lett. **100**, 226403 (2008).
- ⁶J. T. Devreese, S. N. Klimin, J. L. M. van Mechelen, and D. van der Marel, Phys. Rev. B **81**, 125119 (2010).
- ⁷Y. Ishida, R. Eguchi, M. Matsunami, K. Horiba, M. Taguchi, A. Chainani, Y. Senba, H. Ohashi, H. Ohta, and S. Shin, Phys. Rev. Lett. **100**, 056401 (2008).
- ⁸M. Lee, J. R. Williams, S. Zhang, C. D. Frisbie, and D. Goldhaber-Gordon, Phys. Rev. Lett. **107**, 256601 (2011).
- ⁹A. Janotti, J. B. Varley, M. Choi, and C. G. Van de Walle, Phys. Rev. B **90**, 085202 (2014).
- ¹⁰X. Hao, Z. Wang, M. Schmid, U. Diebold, and C. Franchini, Phys. Rev. B **91**, 085204 (2015).
- ¹¹Y. Iwazaki, Y. Gohda, and S. Tsuneyuki, APL Mater. **2**, 012103 (2014).
- ¹²R. Nakayama, M. Maesato, T. Yamamoto, H. Kageyama, T. Terashima, and H. Kitagawa, Chem. Commun. **54**, 12439 (2018).
- ¹³M. D'Angelo, R. Yukawa, K. Ozawa, S. Yamamoto, T. Hirahara, S. Hasegawa, M. G. Silly, F. Sirotti, and I. Matsuda, Phys. Rev. Lett. **108**, 116802 (2012).
- ¹⁴S. Kapphan, J. Koppitz, and G. Weber, Ferroelectrics **25**, 585 (1980).
- ¹⁵G. Weber, S. Kapphan, and M. Wöhlecke Phys. Rev. B **34**, 8406 (1986).
- ¹⁶S. Klauer and M. Wöhlecke, Phys. Rev. B **49**, 158 (1994).
- ¹⁷D. P. Spencer, D. G. Fleming, and J. H. Brewer, Hyperfine Interactions **17-19**, 567 (1984).
- ¹⁸Z. Salman, T. Prokscha, A. Amato, E. Morenzoni, R. Scheuermann, K. Sedlak, and A. Suter, Phys. Rev. Lett. **113**, 156801 (2014).
- ¹⁹S. F. J. Cox, J. L. Gavartin, J. S. Lord, S. P. Cottrell, J. M. Gil, H. V. Alberto, J. Piroto Duarte, R. C. Vilão, N. Ayres de Campos, D. J. Keeble, E. A. Davis, M. Charlton, and D. P. van der Werf, J. Phys.: Condens. Matter **18**, 1079 (2006).
- ²⁰T. U. Ito, W. Higemoto, T. D. Matsuda, A. Koda, K. Shimomura, Appl. Phys. Lett. **103**, 042905 (2013).
- ²¹T. U. Ito, A. Koda, K. Shimomura, W. Higemoto, T. Matsuzaki, Y. Kobayashi, and H. Kageyama, Phys. Rev. B **95**, 020301(R) (2017).
- ²²R. C. Vilão, R. B. L. Vieira, H. V. Alberto, J. M. Gil, A. Weidinger, R. L. Lichti, B. B. Baker, P. W. Mengyan, and J. S. Lord, Phys. Rev. B **92**, 081202(R) (2015).
- ²³K. Shimomura, R. Kadono, A. Koda, K. Nishiyama, and M. Mihara, Phys. Rev. B **92**, 075203 (2015).

- ²⁴A. Amato, H. Luetkens, K. Sedlak, A. Stoykov, R. Scheuermann, M. Elender, A. Raselli, and D. Graf, *Rev. Sci. Instr.* **88**, 093301 (2017).
- ²⁵M. Setvin, C. Franchini, X. Hao, M. Schmid, A. Janotti, M. Kaltak, C. G. Van de Walle, G. Kresse, and U. Diebold, *Phys. Rev. Lett.* **113**, 086402 (2014).
- ²⁶A. Janotti, C. Franchini, J. B. Varley, G. Kresse, and C. G. Van de Walle, *Phys. Status Solidi PRL* **7**, 199 (2013).
- ²⁷S. Yang, A. T. Brant, N. C. Giles, and L. E. Halliburton, *Phys. Rev. B* **87**, 125201 (2013).